Evaluation of the Wharton's jelly poroelastic parameters through compressive tests on placental and foetal ends of human umbilical cords

Francesca Gervaso[a,], Federica Boschetti[a,b], Giancarlo Pennati[a]*

[a]Laboratory of Biological Structure Mechanics, Department of Chemistry, Materials and Chemical Engineering
"Giulio Natta", Politecnico di Milano, Piazza Leonardo da Vinci 32, 20133 Milan, Italy

[b]IRCCS Istituto Ortopedico Galeazzi, Milano, Italy

*Corresponding author. Present address: Department of Engineering for Innovation, University of Salento, Via Monteroni, Lecce 73100, Italy.
Tel.: +39 832297386; fax: +39 832297240.*

E-mail address: francesca.gervaso@unisalento.it (F. Gervaso).

1.   Introduction

The umbilical cord (UC) is a cordlike structure about 50–60 cm in length and 1–2 cm in diameter, extending from the abdominal wall of the foetus to the placenta (that interfaces with the maternal circulation). Its chief function is to carry nourishment and oxygen from the placenta to the foetus and return waste products to the placenta from the foetus. It consists of a continuation of the membrane covering the foetus and encloses a mucoid tissue, the Wharton's jelly (WJ), through which one umbilical vein (UV) carries oxygenated blood and two umbilical arteries (UA) arranged in coils around the vein, carry unoxygenated blood. The Wharton's jelly is a connective mucoid tissue (5% cells, 95% extracellular matrix) rich in water (about 90%), described as a three-dimensional spongy network of interlacing collagen fibres, small woven bundles of glycoprotein micro-fibrils apparently arranged at random.

The umbilical cord, as the lifeline to the foetus, has a crucial importance for foetal well-being and development. In order to guarantee blood flow to the foetus, the umbilical cord structure is required to avoid reduction of the umbilical vessel lumens that may occur as a result of external forces due to foetal movements and uterine contractions. Morphological, histological and biomechanical properties of the cord may influence the susceptibility to vascular occlusion and their abnormal values can be associated with pathologic conditions (i.e. preeclampsia, foetal growth restriction, diabetes, foetal demise).

However, so far, this complex structure has not yet been thoroughly studied from a scientific point of view.

Most of the clinical studies examined the anatomy of the umbilical cord with the aim of correlating the cord morphology (e.g. UC coiling index, UC length and Wharton's jelly area) with the pregnancy outcome (Degani et al., 2001; de Laat et al., 2005, 2006, 2007; Di Naro et al., 2001; Kashanian et al., 2006; Ochshorn et al., 2009; Peng et al., 2006; Raio et al., 2003; Togni et al., 2007). Furthermore, numerous studies investigated the ultra-structure of either umbilical cord arteries and vein (Cetin et al., 2002; Sexton et al., 1996; Stehbens et al., 2005) or matrix in healthy or pathologic cases (Franc et al., 1998; Gogiel et al., 2003, 2005; Romanowicz and Bańkowski, 2010a, 2010b)).

However, although an extremely sophisticated mechanism of protection of the umbilical vessels against external forces is expected, detailed biomechanical data are still lacking. As underlined in a recent review by Ferguson and Dodson (2009), the literature concerning the mechanics of the umbilical cord is inadequate despite the fact that biomechanical studies would be very important to understand the function of tissues of normal and pathological umbilical cords.

The UC is subjected *in utero* to torsion, traction, compression and bending due to foetal movements or cord encirclement around foetal body parts (mainly nuchal); moreover, cord compression is associated to uterine contractions. Previous studies investigated the biomechanics of whole UC, measuring tensile properties (Ghosh et al., 1984) and assessing the variation of the umbilical vein flow due to mechanical loading as compression, twisting and longitudinal stretching (Dado et al., 1997). Furthermore, Georgiou et al. (2001) evaluated the venous perfusion in umbilical cords subjected to a standardized tight encirclement force, comparing cords from normal pregnancies and those complicated by gestational diabetes mellitus and intrauterine growth restriction. Recently, Pennati et al. (2013) investigated the hydraulic behaviour of the umbilical vein during different cord compressions, suggesting a quite peculiar non linear response: amazingly, for high cord compressions, the pressure drop decreases when the flow rate increases. A possible role of WJ mechanical response due to its poroelastic behaviour was suggested to explain this occurrence, although the specific mechanism acting during cord compression was not demonstrated.

Referring to other poroelastic structures, finite element modelling was applied to give insight into complex biomechanical behaviours of (e.g. Gupta et al., 2009; Chagnon et al., 2010). Numerical models, though, require, the measurement of the mechanical properties of UC components and the definition of proper constitutive material models to be implemented.

The mechanical behaviour of umbilical vessels has been investigated by several authors. Bertrand et al. (1993) analysed tensile properties of both arteries and veins in circumferential direction; Hellevik et al. (1998) and Li et al. (2006) tested the umbilical veins in circumferential directions as a basis for describing the pulse wave propagation and as optional material for grafting, respectively; Pennati (2001) reported the mechanical behavior of umbilical veins both in circumferential and longitudinal direction. Conversely, a single study investigated the biomechanics of WJ, measuring its tensile stiffness and viscoelasticity (Pennati, 2001).

WJ reduction has been invoked as a possible cause of foetal complications (Di Naro et al., 2001). Peng et al. (2006) reported that a localized deficiency of Wharton's jelly and an increase in collagen content can be found in all cases of umbilical cord stricture that has been established as one of the main causes of intrauterine foetal demise. The Wharton's jelly is hence expected to play a key role in sustaining compressive loads.

In the present study the biomechanics of the human WJ under compression are investigated, since compressive stresses are expected in vivo as a consequence of either compression, bending or torsion forces, and could compromise the pregnancy outcome (Baergen, 2007; Takahashi et al., 2006). Moreover, since differences may occur in mechanical properties of different segments as observed for coiling index (Blickstein et al., 2001), measurements are performed on samples obtained from foetal and placental ends. In particular, since WJ is extremely rich of water, a poroelastic approach is adopted and multi-ramp confined and unconfined compression tests are performed in order to obtain material parameters.

2.   Materials and methods

2.1.   *Sample preparation*

Twenty umbilical cords were collected from term Caesarian deliveries, after uncomplicated pregnancies, at the Obstetric Unit of the Department of Clinical and Biological Sciences of

the University of Milan, Italy. Institutional review board approval was obtained at the hospital. All women who donated cord specimen for research did so voluntarily after giving informed consent. During surgery the complete placenta-cord system was extracted, according to the normal medical procedure. A cord segment of roughly 30 cm was excised, blood was heparinized and expressed from both umbilical arteries and vein to avoid clot formation; UC was then immersed in phosphate buffered saline (PBS: 0.15 mmol/l NaCl; 1.54 mmol/l NaH_2PO_4; 2.71 mmol/l Na_2HPO_4, purchased from Sigma-Aldrich Srl, Milan, Italy) containing protease inhibitors (PI: 1 mmol/l phenylmethyl-sulfonyl-fluoride; 2 mmol/l EDTA; 5 mmol/l benzamidine; 10 mmol/l N-ethyl-maleimide, purchased from Sigma-Aldrich Srl, Milan, Italy) and transported to the laboratory.

Half of the cords were used for preliminary tests, necessary to define the testing protocol. The preliminary tests were performed to assess (i) the necessity of WJ preconditioning, (ii) the recovery time, (iii) the possibility of freezing samples without significant changes in mechanical properties (iv) an estimate of the tissue strain state corresponding to in utero conditions and (v) the completion of relaxation. In summary, the preliminary test results (data not reported) showed that: (i) the conditioning of the tissue can be fully reached after 12 cycles; (ii) an elapsing time of 4 h between two tests on the same sample is enough to take the tissue back to its initial condition; (iii) WJ can be properly stored at $-27\,°C$; (iv) after a creep test at 2 kPa (i.e. 15 mmHg, corresponding to the UV pressure) a strain of about 40% was measured; (v) the asymptotic value of the stress was reached after about 20 min (ratio between stresses measured at 17 and 20 min was approximately equal to 1 (Pennati, 2001)).

The umbilical cords subjected to the testing protocol ($n=10$) were cut in two parts (labelled as foetal and placental according to their position, Fig.1a) about 12 cm long and frozen at $-27\,°C$.

At the time of mechanical testing, from each part of the frozen cord three slices of about 1 mm of thickness were cut off with a custom microtome and a disk of 5 mm was obtained by punching in the cord region free of vessel lumens or walls (Fig.1b). Two of the four slices were used for compression tests and one for porosity measurements. The remaining cord tissue was kept frozen for further investigations, not reported in the present study.

2.2. Compression test and porosity measurements

According to the expected biphasic behaviour of WJ and to preliminary test results, confined and unconfined compression tests were performed following a protocol similar to the one previously developed for articular cartilage (Boschetti et al., 2006). The protocol consists of the following steps: (a) thickness measurement, (b) tissue preconditioning, (c) tissue preloading to physiological conditions, (d) multi-ramp unconfined compression stress–relaxation test, (e) tissue recovery, (f) multi-ramp confined compression stress–relaxation test (repeating steps a–c).

First, the sample was placed between the two stainless steel plates of a testing machine (Bose ELF 3200) equipped with a 22 N loading cell and a constant force of 0.01 N was applied in order to guarantee a uniform contact with the specimen; the load was maintained until a constant displacement was reached and the corresponding distance between the two plates was recorded and assumed as the thickness of the sample (h_{sample}). Subsequently, twelve cycles of preconditioning up to 40% strain were executed at a 0.01 mm/s cross-head velocity, then the 40% strain was kept for 20 min as a physiological preload: the imposed preload was necessary since the Wharton's jelly exhibits a significant material non-linearity (Pennati, 2001) and the present tests aimed to evaluate WJ mechanical response to external loads in in utero conditions. Finally, three further unconfined compression ramps of 5% strain (referred to initial specimen thickness) each followed by 20 min of relaxation, were performed.

At the end of the unconfined test, the samples were immersed in the PBS+PI for 4 h according to the recovery test results. The confined compression was performed placing the sample in a confining chamber with a porous floor filled with PBS+PI and using the same protocol of the unconfined test.

The cord slices were deprived of the amniotic cover and the vessel walls in order to obtain the porosity of the sole jelly component. The hydrated specimens were weighed with an analytical balance (Sartorius, resolution: 10^{-5} g), dried in oven at 40 °C for 48 h and weighed again.

The porosity was then calculated using the following

$$\varphi = \frac{V_{wet} - V_{dry}}{V_{wet}} = \frac{W_{wet} - W_{dry}}{W_{wet}}$$
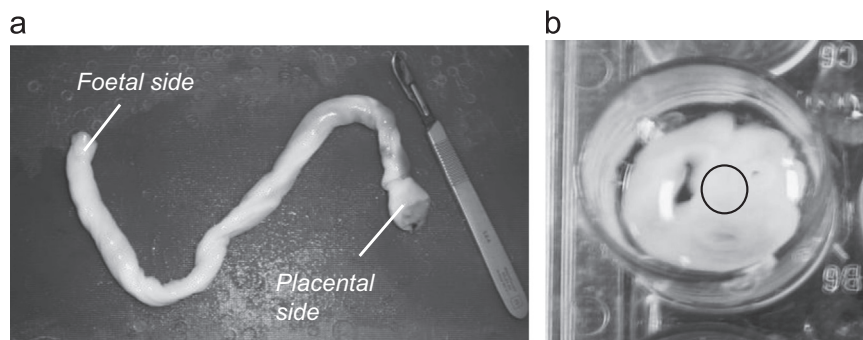

a

b

Foetal side

Placental side

Fig. 1 – (a) Umbilical cord before samples preparation; the cord is cut in two parts labelled as foetal and placental according to their position; (b) umbilical cord slice; the black circle in the picture indicates the area among the three vessels punched to obtain the 5 mm diameter Wharton's jelly specimen.

where V and W are respectively the volume and the weight of the sample in the wet and dry state and assuming the Wharton's jelly density equal to the water one, since a porosity around 95% is expected (Sloper et al.,1979).

2.3.   Poroelastic model of WJ

The linear biphasic media theory (Mow et al., 1980) was adopted to describe the Wharton's jelly mechanical compressive behaviour. The Wharton's jelly was modelled as a composite material consisting of two phases, a solid matrix representing the extra-cellular matrix, and a fluid. The solid phase was assumed incompressible and two parameters, the Young modulus (E) and the Poisson ratio (v) describe its isotropic linear elastic behaviour. The fluid is incompressible and its interaction with the solid matrix is represented by the hydraulic permeability K.

Using the equilibrium stress–strain data of the unconfined and confined compression tests, the Young modulus (E) and the aggregate modulus (H_A) were respectively calculated as the ratio between the asymptotic stress values and the imposed strain values. From E and H_A values, the Poisson ratio can be analytically calculated inverting the following relation:

$$H_A = \frac{E(1-v)}{(1+v)(1-2v)}$$

The hydraulic permeability values (K) were found by fitting the confined stress–relaxation data to the analytical solution and minimizing the least square differences in stress.

The confined stress–relaxation analytical solution based on the linear biphasic theory was implemented and used to simulate the confined stress–relaxation test:

$$\sigma_z(t) = H_A \dot{\varepsilon}_0 h_{sample}^2 \left(\frac{t}{h_{sample}^2} + \frac{1}{3H_A K} - 2\frac{1}{\pi^2 H_A K} \sum_{n=1}^{\infty} \frac{e^{\frac{-n^2\pi^2 H_A K}{h_{sample}^2}t}}{n^2} \right) \, for \, (t < t_0),$$

$$\sigma_z(t) = H_A \dot{\varepsilon}_0 h_{sample}^2 \left(\frac{t_0}{h_{sample}^2} - \frac{2}{\pi^2 H_A K} \sum_{n=1}^{\infty} \frac{e^{\frac{-n^2\pi^2 H_A K t}{h_{sample}^2}} - e^{\frac{-n^2\pi^2 H_A K(t-t_0)}{h_{sample}^2}}}{n^2} \right) \, for \, (t > t_0),$$

Where $\dot{\varepsilon}_0$ is the strain rate and t_0 is the load phase time.

In order to best-fit the data, the least squares method was used. According to this method, the parameters of the model function are adjusted in order to best fit the experimental data set. The best-fit will be reached when the sum (S) of squared residuals reaches its minimum, a residual (r) being the difference between the experimental value and the fitted value provided by the model.

$$S = \sum_{i=1}^{n} r_i^2$$

$$r_i = y_i - f(x_i\beta)$$

The value of the permeability K was estimated for each single ramp and then expressed as a function of strain.

2.4.   Statistical analysis

For each cord the poroelastic properties of sixty WJ samples were investigated. Twenty samples for each cord extremity
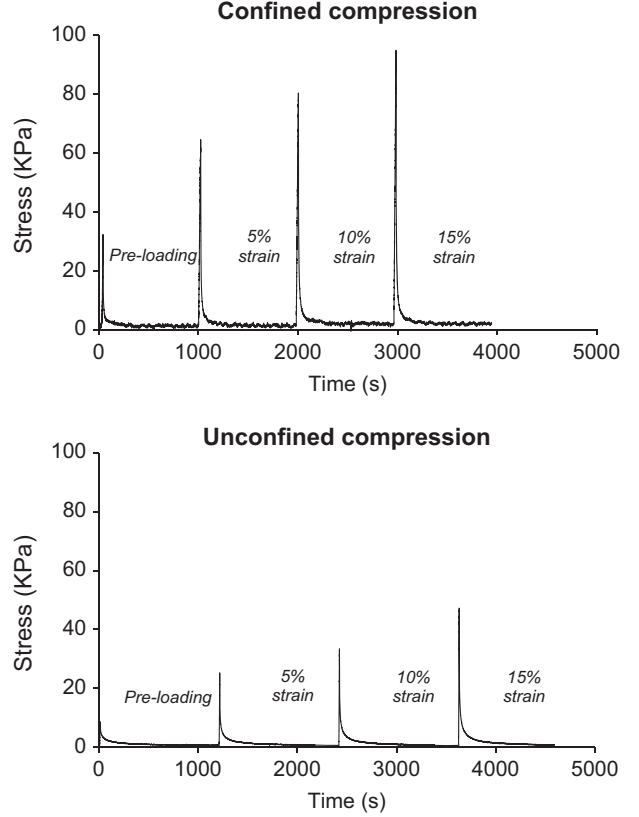

Fig. 2 – Stress–relaxation response to compression test in the confined and unconfined configuration for two WJ samples.

underwent compression tests and ten samples for each side were used for the porosity measurement. The percentage of stress relaxation was calculated as the difference between the peak stress and equilibrium stress divided by the peak stress. The values of the measured and calculated parameters (H_A, E, ν, K, ϕ) are reported as mean ± standard deviation. The mechanical parameters of the foetal side were compared to those of the placental side by t-test and the differences were considered significant when $p < 0.05$.

3.   Results

The umbilical cord slices had an average thickness of 1.2 ± 0.2 mm, the resulting strain rate used in the test was therefore equal to $0.0083 \, s^{-1}$.

Ten WJ samples for each umbilical cord side were weighted both in wet and dry state. The porosity resulted equal to $93.5 \pm 1.7\%$ and $88.3 \pm 6.0\%$ for foetal and placental ends respectively ($n = 10$ each side). The porosity at the foetal end is therefore slightly higher than the porosity at the placental end (significant difference, $p = 0.014$).

In Fig. 2 the confined and unconfined compression responses for two samples are shown. The material exhibits a transient stress–relaxation behaviour to the applied displacement in both test configurations and is highly viscoelastic showing a percentage of relaxation of $\sim 90\%$ and $\sim 85\%$ in the unconfined and confined configurations, respectively.
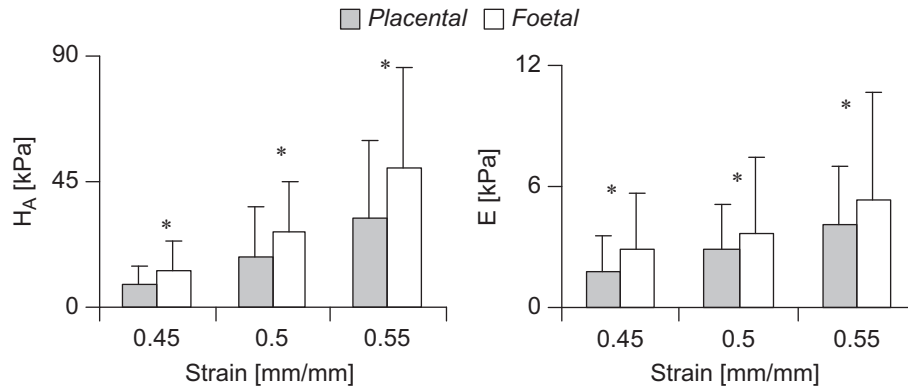
Fig. 3 – The mean values of the Aggregate (H_A) and Young modulus (E) for the placental (grey) and foetal (white) Wharton's jelly samples at three different strain values. *Significant differences between the two sides ($p < 0.05$).
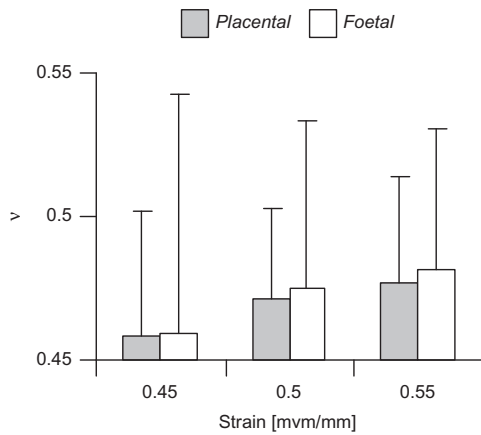

Fig. 4 – The mean values of the Poisson ratio for the placental (grey) and foetal (white) Wharton's jelly samples at three different strain values.
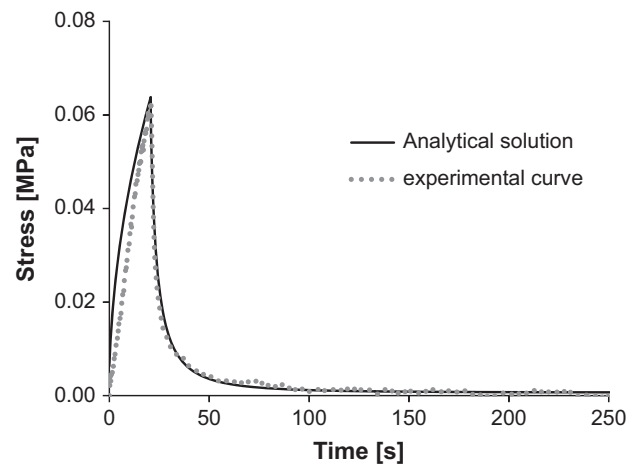

Fig. 5 – The fitting of a single stress–relaxation ramp by the analytical solution.

The equilibrium stress is reached in about 5 min in the confined compression and in about 15 min in the unconfined test. Moreover, in order to evaluate the stress relaxation time in the two test configurations, the time at which the stress reaches the 70% of its peak value was calculated for both confined and unconfined compression. According to this criteria, the stress relaxation time of the unconfined compression results almost triple of the stress relaxation time of the confined compression. Since the differences between the stress–relaxation times of the two test configuration was considerable, none statistical analysis was performed.

As expected, the peak stress in the confined configuration is significantly higher than in the unconfined one where the sample is free to expand radially.

The values of H_A and E were calculated for each sample at the three imposed strains and their averages and the standard deviation at both foetal and placental sides are reported in Fig. 3. The two moduli increase with strain and, for both of them, the placental side values are significantly lower than the foetal side for each strain value ($p < 0.05$). The Poisson ratio was analytically calculated from measured H_A and E

values. However the coefficient of variance for these data is so high that a possible influence of the strain value on this parameter cannot be postulated. (Fig. 4). The fitting of a single stress–relaxation ramp by the analytical solution is reported in Fig.5: the adopted poroelastic model could properly fit the experimental data. The values of the permeability, K, calculated for each single ramp are reported for foetal and placental sides in Fig. 6; the permeability values decrease with strain, as expected, and this behaviour is more emphasised for the placental side. Although the foetal side values are lower at every strain value analysed, the differences were statistically significant only at the lowest strain value (i.e. 45%).

4. Discussion

A protocol for testing the Wharton's jelly of the umbilical cord in compression was successfully developed; a poroelastic approach was followed that allowed the estimation of the WJ compressive poroelastic parameters. The porosity of the
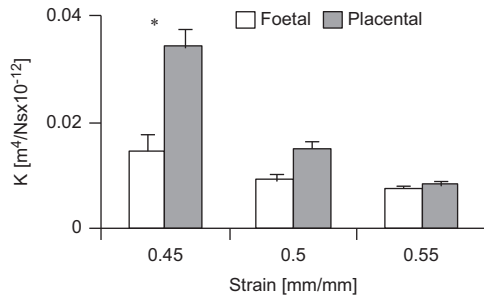
Fig. 6 – The mean permeability values for the two umbilical cord sides (foetal and placental) from the stress–relaxation experiment curve-fitting. *Significant difference between placental and foetal side ($p < 0.05$).

WJ was properly measured and the obtained mean porosity values are in agreement with the literature results (Sloper et al., 1979).

Stress–relaxation multi-ramp confined and unconfined tests were successfully performed on Wharton's jelly samples excised from both placental and foetal side of ten frozen umbilical cords.

In order to evaluate the freezing effect on the mechanical properties of the Wharton jelly samples, preliminary tests have been performed. Five samples underwent stress–relaxation test after and before freezing ($-27\,°C$ for 48 h). The results were analysed in terms of peak and relaxation force values ratio between post- and pre-freezing. The differences between the two tested situations were not significant, therefore we assumed that the Wharton's jelly can be stored at $-27\,°C$ without inducing significant variations in its biomechanical properties. We would like to underline that, as reported by other authors (ref), the freezing do effect the biochemical analysis of some biological tissues. However, Chow and Zhang (2011), for example, in their study on the aortic tissue, showed that freezing influences the biochemical composition but does not influence the mechanical properties. Our study on Wharton's jelly was focused on the mechanical properties of the tissue and none biochemical analysis was performed. Therefore, the freezing influence on the mechanical properties only was assessed.

The material shows a marked viscoelastic behaviour. In the present study the WJ matrix was assumed linear elastic, therefore, the WJ viscoelasticity was attributed merely to the water movements through the spongy network of collagen fibres and glycoproteins micro-fibrils. From the stress–relaxation curves it could be noticed that the WJ reaches the equilibrium stress faster in the confined configuration than in the unconfined configuration. During confined compression, the sample lies on a porous filter and its lateral expansion is avoided by the confining chamber, therefore the water movement is uniquely in the axial direction. Conversely, during unconfined compression, the sample is compressed between two impermeable plates, it can freely expand radially and water moves predominantly in the radial direction. According to these considerations and in the hypothesis of considering only the fluid-dependent viscoelasticity, it could be hypothesised that the permeability of the

Wharton's jelly is not isotropic. Therefore, since the axial direction of the sample in the compression test is also the axial direction of the umbilical cord it could also be speculated that the permeability of the WJ in the radial direction is lower than the permeability along umbilical cord axis. The peak stress is of course influenced by the test configuration and, as expected, it is higher in the confined compression in which the sample is not free to expand radially. The confined and unconfined compression experiments allowed to obtain the three compression parameters (H_A, E, K), according to the poroelastic model. To the best of our knowledge, up to date, the data reported in the present study are the first available on the compressive properties of Wharton's jelly, therefore a comparison with literature is not possible. However, we can hypothesize that the relatively high peak stress values could be necessary to contrast possible not desired, usually rapid, foetal movements. On the contrary, the very low stress at equilibrium could be due to allow the regular vessel wall motion due to the blood pressure occurring in a very long time scale. These suppositions suggest that the Wharton's jelly plays an important role in the protection mechanism of the foetus during pregnancy.

A dependence of the three material parameters (H_A, E, K) on the position (foetal and placental side) was observed, showing a non-homogeneity in the mechanical properties of the tissue. According to our results, the Young modulus and the Aggregate modulus at equilibrium are significantly higher at the foetal side where, conversely, the permeability is significantly lower. However, although significant differences were detected between the distal and proximal Wharton's jelly compression parameters, a consistent interpretation of these findings is very arduous to carry on. Li et al (2006) investigated the differences between foetal and placental morphology and mechanical properties of the umbilical cord vessels walls only, therefore, again a precise comparison of our results with the literature is not possible. Nevertheless, they found a significant changes between the umbilical vein extracted at the two cord extremities, with higher stiffness at the foetal end. This is in agreement with our findings for the WJ. In order to give a reliable explanation of the reasons why WJ shows non-homogeneous mechanical properties, further investigations are needed. Future work on the topic will include a second set of experimental tests (such as SEM observation and ECM biochemical analyses) with the purpose of correlating the WJ mechanical properties to the WJ composition. Hopefully, the future findings will help to understand why the compressive poroelastic parameters of the foetal side of the umbilical cord are significantly different from the placental side.

As already underlined above, in the present study, the hydraulic permeability was estimated fitting the experimental data to the analytical solution that considers the matrix linear elastic. In our simplified model the estimated permeability is purely attributed to the fluid movements through the WJ matrix fibers. Actually, the matrix could also be intrinsically viscoelastic. The permeability we estimated would be, in this case, a "global value" not able to discriminate between the fluid-dependent viscoelastic contribution and the intrinsic viscoelastic contribution. In order to verify the WJ matrix nature, a direct measurement

of the hydraulic permeability should, therefore, be performed and a comparison between the measured and estimated values carried out.

5. Conclusions

The mechanical properties in compression of the Wharton's jelly of the umbilical cord were investigated. A poroelastic approach was adopted that considered the WJ a biphasic material made of a linear elastic incompressible solid phase and of an incompressible fluid phase. According to the adopted biphasic model, the poroelastic parameters H_A, E, K and their dependence on the umbilical cord location (foetal or placental side) were properly evaluated. The estimated parameters showed a strong dependence on the strain value applied and on the position suggesting the existence of a correlation between the WJ composition and the UC function that requires further investigations.

REFERENCES

Baergen, R.N., 2007. Cord abnormalities, structural lesions, and cord "accidents". Semin. Diagn. Pathol. 24 (1), 23–32.

Bertrand, C., Duperron, L., St-Louis, J., 1993. Umbilical and placental vessels: modifications of their mechanical properties in preeclampsia. Am. J. Obstet. Gynecol. 168 (5), 1537–1546.

Blickstein, I., Varon, Y., Varon, E., 2001. Implications of differences in coiling indices at different segments of the umbilical cord. Gynecol. Obstet. Invest. 52 (3), 203–206.

Boschetti, Federica, Gervaso, Francesca, Pennati, Giancarlo, Peretti, Giuseppe M., Vena, Pasquale, Dubini, Gabriele, 2006. Poroelastic numerical modelling of natural and engineered cartilage based on in vitro tests. Biorheology 43, 235–247.

Cetin, A., Kukner, A., Ozturk, F., 2002. Ultrastructure of human umbilical vessels in pre-eclampsia. J. Matern. Fetal Neonatal Med. 12 (3), 178–184.

Chagnon, A, Aubin, C.E., Villemure, I., 2010. Biomechanical influence of disk properties on the load transfer of healthy and degenerated disks using a poroelastic finite element model. J. Biomech. Eng. 132 (11), 111006.

Chow, M., Zhang, Y., 2011. Changes in the mechanical and biochemical properties of aortic tissue due to cold storage. J. Surg. Res. 171 (2), 434–442.

Dado, G.M., Dobrin, P.B., Mrkvicka, R.S., 1997. Venous flow through coiled and noncoiled umbilical cords. Effects of external compression, twisting and longitudinal stretching. J. Reprod. Med. 42 (9), 576–580.

Degani, S., Leibovich, Z., Shapiro, I., Gonen, R., Ohel, G., 2001. Early second-trimester low umbilical coiling index predicts small-for-gestational-age fetuses. J. Ultrasound Med. 20 (11), 1183–1188.

de Laat, M.W., Franx, A., van Alderen, E.D., Nikkels, P.G., Visser, G.H., 2005. The umbilical coiling index, a review of the literature. J. Matern. Fetal Neonatal Med. 17 (2), 93–100.

de Laat, M.W., Franx, A., Nikkels, P.G., Visser, G.H., 2006. Prenatal ultrasonographic prediction of the umbilical coiling index at birth and adverse pregnancy outcome. Ultrasound Obstet. Gynecol. 28 (5), 704–709.

de Laat, M.W., van Alderen, E.D., Franx, A., Visser, G.H., Bots, M.L., Nikkels, P.G., 2007. The umbilical coiling index in complicated pregnancy. Eur. J. Obstet. Gynecol. Reprod. Biol. 130 (1), 66–72.

Di Naro, E., Ghezzi, F., Raio, L., Franchi, M., D'Addario, V., 2001. Umbilical cord morphology and pregnancy outcome. Eur. J. Obstet. Gynecol. Reprod. Biol. 96 (2), 150–157.

Ferguson, V.L., Dodson, R.B., 2009. Bioengineering aspects of the umbilical cord. Eur. J. Obstet. Gynecol. Reprod. Biol. 144 (Suppl. 1), S108–S113.

Franc, S., Rousseau, J.C., Garrone, R., van der Rest, M., Moradi-Améli, M., 1998. Microfibrillar composition of umbilical cord matrix: characterization of fibrillin, collagen VI and intact collagen V. Placenta 19 (1), 95–104.

Georgiou, H.M., Rice, G.E., Walker, S.P., Wein, P., Gude, N.M., Permezel, M., 2001. The effect of vascular coiling on venous perfusion during experimental umbilical cord encirclement. Am. J. Obstet. Gynecol. 184 (4), 673–678.

Ghosh, K.G., Ghosh, S.N., Gupta, A.B., 1984. Tensile properties of human umbilical cord. Indian J. Med. Res. 79, 538–541 (Apr).

Gogiel, T., Bańkowski, E., Jaworski, S., 2003. Proteoglycans of Wharton's jelly. Int. J. Biochem. Cell Biol. 35 (10), 1461–1469.

Gogiel, T., Galewska, Z., Jaworski, S., 2005. Pre-eclampsia-associated alterations in Wharton's jelly proteoglycans. Acta Biochim. Pol. 52 (2), 501–507.

Gupta, S., Lin, J., Ashby, P., Pruitt, L., 2009. A fiber reinforced poroelastic model of nanoindentation of porcine costal cartilage: a combined experimental and finite element approach. J. Mech. Behav. Biomed. Mater. 2 (4), 326–337.

Hellevik, L.R., Kiserud, T., Irgens, F., Stergiopulos, N., Hanson, M., 1998. Mechanical properties of the fetal ductus venosus and umbilical vein. Heart Vessels 13 (4), 175–180.

Kashanian, M., Akbarian, A., Kouhpayehzadeh, J., 2006. The umbilical coiling index and adverse perinatal outcome. Int. J. Gynaecol. Obstet. 95 (1), 8–13.

Li, W.C., Ruan, X.Z., Zhang, H.M., Zeng, Y.J., 2006. Biomechanical properties of different segments of human umbilical cord vein and its value for clinical application. J. Biomed. Mater. Res. Part B 76 (1), 93–97.

Mow, V.C., Kuei, S.C., Lai, W.M., Armstrong, C.G., 1980. Biphasic creep and stress relaxation of articular cartilage in compression. Theory and experiments. J. Biomech. Eng. 102 (1), 73–84.

Ochshorn, Y., Bibi, G., Ascher-Landsberg, J., Kupferminc, M.J., Lessing, J.B., Many, A., 2009. Coiling characteristics of umbilical cords in breech vs. vertex presentation. J. Perinat. Med. 37 (5), 525–528.

Peng, H.Q., Levitin-Smith, M., Rochelson, B., Kahn, E., 2006. Umbilical cord stricture and overcoiling are common causes of fetal demise. Pediatr. Dev. Pathol. 9 (1), 14–19.

Pennati, G., 2001. Biomechanical properties of the human umbilical cord. Biorheology 38 (5-6), 355–366.

Pennati, G., Laganà, K., Gervaso, F., Rigano, S., Ferrazzi, E., 2013. How do cord compressions affect the umbilical venous flow resistance? An in vitro investigation of the biomechanical mechanisms. Cardiovasc. Eng. Tech. 4 (3), 267–275.

Raio, L., Ghezzi, F., Di Naro, E., Duwe, D.G., Cromi, A., Schneider, H., 2003. Umbilical cord morphologic characteristics and umbilical artery Doppler parameters in intrauterine growth-restricted fetuses. J. Ultrasound Med. 22 (12), 1341–1347.

Romanowicz, L., Bańkowski, E., 2010a. Lipid compounds of human Wharton's jelly and their alterations in preeclampsia. Int. J. Exp. Pathol. 91 (1), 1–9.

Romanowicz, L., Bańkowski, E., 2010b. Altered sphingolipid composition in Wharton's jelly of pre-eclamptic newborns. Pathobiology 77 (2), 78–87.

Sexton, A.J., Turmaine, M., Cai, W.Q., Burnstock, G., 1996. A study of the ultrastructure of developing human umbilical vessels. J. Anat. 188, 75–85.

Sloper, K.S., Brown, R.S., Baum, J.D., 1979. The water content of the human umbilical cord. Early Hum. Dev. 3 (2), 205–210.

Stehbens, W.E., Wakefield, J.S., Gilbert-Barness, E., Zuccollo, J.M., 2005. Histopathology and ultrastructure of human umbilical blood vessels. Fetal Pediatr. Pathol. 24 (6), 297–315.

Takahashi, T., Sugawara, J., Chisaka, H., Imai, N., Saito, M., Murakami, T., Kimura, Y., Okamura, K., 2006. Appearance of abnormal electrocorticogram patterns during umbilical cord compression in sheep fetus. Tohoku J. Exp. Med. 208 (1), 9–17.

Togni, F.A., Araujo Júnior, E., Vasques, F.A.P., Moron, A.F., Torloni, M.R., Nardozza., L.M.M., 2007. The cross-sectional area of umbilical cord components in normal pregnancy. Int. J. Gynecol. Obstet. 96, 156–161.